Check for updates

ARTICLE

Unsynchronized butyrophilin molecules dictate cancer cell evasion of Vγ9Vδ2 T-cell killing

Zeguang Wu[1,7], Qiezhong Lamao[1,7], Meichao Gu[1,7], Xuanxuan Jin[1], Ying Liu[1], Feng Tian[1], Ying Yu[1], Pengfei Yuan[2], Shuaixin Gao[3], Thomas S. Fulford[4], Adam P. Uldrich[4,5], Catherine CL Wong[6✉] and Wensheng Wei[1✉]

Vγ9Vδ2 T cells are specialized effector cells that have gained prominence as immunotherapy agents due to their ability to target and kill cells with altered pyrophosphate metabolites. In our effort to understand how cancer cells evade the cell-killing activity of Vγ9Vδ2 T cells, we performed a comprehensive genome-scale CRISPR screening of cancer cells. We found that four molecules belonging to the butyrophilin (BTN) family, specifically BTN2A1, BTN3A1, BTN3A2, and BTN3A3, are critically important and play unique, nonoverlapping roles in facilitating the destruction of cancer cells by primary Vγ9Vδ2 T cells. The coordinated function of these BTN molecules was driven by synchronized gene expression, which was regulated by IFN-γ signaling and the RFX complex. Additionally, an enzyme called QPCTL was shown to play a key role in modifying the N-terminal glutamine of these BTN proteins and was found to be a crucial factor in Vγ9Vδ2 T cell killing of cancer cells. Through our research, we offer a detailed overview of the functional genomic mechanisms that underlie how cancer cells escape Vγ9Vδ2 T cells. Moreover, our findings shed light on the importance of the harmonized expression and function of gene family members in modulating T-cell activity.

INTRODUCTION

Vγ9Vδ2 T cells serve as sentinels that survey the surrounding environment for cells infected by pathogens and for transformed cells with imbalanced phosphoantigen (pAg) biosynthesis [1]. These T cells can eliminate various cancer cells [2]. Nevertheless, the genetic factors that contribute to cancer cell evasion of the cytotoxic effects of Vγ9Vδ2 T cells, including those targeted by therapeutics, are poorly understood.

As members of the B7 immunoglobulin superfamily that are widely expressed in cancer cells [3], BTN2A1 and BTN3A1 are crucial molecular facilitators of the anticancer activity of Vγ9Vδ2 T cells [4–7]. In particular, BTN2A1 has been shown to directly interact with germline-encoded regions of the Vγ9 T-cell receptor (TCR) in a manner that is independent of pAg exposure [4]. In contrast, direct interactions between BTN3A1 and the TCR on Vγ9Vδ2 cells have not been detected via transfection assays [5]. Nonetheless, experiments involving site-directed mutagenesis of either Vγ9Vδ2 TCR [4] or BTN3A1 [8] revealed that such mutations abolished TCR responsiveness in Vγ9Vδ2 cells in the presence of BTN2A1. This finding

suggested that there may be an unidentified molecule(s) present on either the target or T cells that are involved in recognition by the Vγ9Vδ2 cell TCR and that act as synergistic partners [9].

PAgs are initiators of Vγ9Vδ2 T-cell activation. These small pyrophosphate metabolites are found in cells infected by pathogens and in malignant target cells. The activation of BTN3A1 in cancer cells depends on the increased availability of isopentenyl diphosphate (IPP), a particular type of cellular pAg. The concentration of IPP can be increased through treatment with bisphosphonate drugs (BPs), which can inhibit farnesyl pyrophosphate synthase (FPPS), an enzyme involved in the mevalonate pathway. This inhibition leads to the accumulation of IPP within the cell.

A few bisphosphonate drugs have been approved for treating bone disorders, particularly osteoporosis and metastatic bone cancers, by inhibiting osteoclasts to alleviate bone material loss. The intracellular B30.2 domain of BTN3A1 is critical for binding pAg, interacting with BTN2A1, and inducing a change in the conformation of its extracellular domain. This leads to the

assembly of various components that activate Vγ9Vδ2 T cells [4, 5, 10, 11], suggesting that small molecules that initiate "inside-out" signaling are key for the activation of Vγ9Vδ2 T cells by BTN molecules.

Cancer cells treated with clinically relevant drugs, such as zoledronic acid (ZOL), were found to be susceptible to elimination by Vγ9Vδ2 T cells [12]. A clinical trial demonstrated the anticancer effects of using expanded Vγ9Vδ2 T cells combined with ZOL [13]. Furthermore, ZOL-conjugated therapeutic antibodies designed to target cancers by engaging Vγ9Vδ2 T cells [14]. Nonetheless, the exact mechanisms by which ZOL enters cancer cells and its intracellular transport have not been determined.

Vγ9Vδ2 T cells hold a significant position in immunotherapy and possess certain advantages in regard to biological engineering. For instance, these cells rarely cause graft-versus-host disease (GVHD), and they exhibit rapid reconstitution following stem-cell transplantation [15]. In our study, we explored and described the genomic landscape involved in cancer cells evasion of destruction by Vγ9Vδ2 T cells. Moreover, we demonstrated the indispensable and unique roles of four BTN molecules in activating Vγ9Vδ2 T cells.

RESULTS
Identifying the functional genetic determinants of cancer cell escape from Vγ9Vδ2 T-cell destruction
Gamma delta T cells are detectable in cancer tissues and have been associated with favorable clinical outcomes in patients with solid tumors [16]. In addition, treatment with BTN3A agonist antibodies has been shown to promote the infiltration of Vγ9^{+} T cells into melanoma tissues, suggesting that the direct anticancer effect of these agents is attributable to gamma delta T cells [17]. Since BTN2A1 and BTN3A1 play critical roles in the activation of Vγ9Vδ2 T cells, we performed a correlation analysis using gene expression data from patients with melanoma. The findings demonstrated a positive correlation between two BTN molecules and overall survival in melanoma patients (Fig. 1A). Encouraged by these findings, we used A375 melanoma cells to investigate the genomic factors that enable cancer cells to evade destruction by Vγ9Vδ2 T cells (Fig. 1B).

After confirming that Vγ9Vδ2 T cells were responsive to A375 cells exposed to ZOL (termed A375-ZOL) (Fig. 1C), we proceeded with genome-wide positive CRISPR screens, in which only the perturbed cells that developed resistance to T-cell killing were enriched. We utilized an optimized library that contained sgRNAs with multiple internal barcodes (iBARs) with improved efficiency and accuracy [18]. Library-transduced Cas9-expressing A375 cells were either propagated continually or challenged with expanded Vγ9Vδ2 T cells (Fig. 1D). Specifically, A375 cells were subjected to two rounds of challenge with Vγ9Vδ2 T cells at an effector T-cell-to-target T-cell (E:T) ratio of 1:4. After each challenge, the suspended T cells were removed, and the target cells were allowed to recover for one week. The abundance of sgRNAs relative to that in the control group that was not treated was subsequently determined via deep sequencing (Fig. 1D). The screening results were consistent when analyses were performed based on varying ratios of effector T cells to target T cells (E:T), which ranged from 1:4 to 1:1 (Fig. 1E and Supplementary Fig. S1A, B).

To investigate the generalizability of the genetic determinants identified, we performed an additional genome-wide CRISPR screening with K562 cells. Notably, Vγ9Vδ2 T cells responded to ZOL-treated K562 (K562-ZOL) cells to a lesser extent than they did to A375 cells (Fig. 1C). The optimal concentrations of ZOL and effector T-cell-to-target T-cell (E:T) ratios were established using a killing assay. This assay showed that 75% of K562 cells were lysed at an E:T ratio of 1:2, whereas 90% were lysed at an E:T ratio of 1:1 (Supplementary Fig. S1C). SgRNA-transduced Cas9-expressing K562 cells were either propagated normally or challenged with

expanded Vγ9Vδ2 T cells using the same screening pipeline (Fig. 1D). Through this screening, SLC37A3 and four BTN molecules emerged as the top hits, and disruption of their expression promoted K562-ZOL cell survival even in the presence of Vγ9Vδ2 T cells (Fig. 1F).

Functionally synchronized BTN2A1/BTN3A1/BTN3A2/BTN3A3 enable Vγ9Vδ2 T-cell killing of cancer cells
We next validated a panel of hits from both screening experiments by performing a competitive killing assay. In this assay, we mixed mCherry-tagged knockout cells with GFP-tagged control cells and evaluated the relative enrichment of mCherry-positive cells following Vγ9Vδ2 T-cell treatment; the results were compared with those of the untreated groups. BTN2A1, BTN3A1, BTN3A3, and BTN3A2 emerged as the dominant genes across all the independent screens. Remarkably, the deletion of any of these four BTN molecules protected cancer cells from Vγ9Vδ2 T-cell-mediated killing. These findings imply that these molecules play vital and nonredundant roles (Fig. 1G). We further tested 14 genes in A375 cells and 13 genes in K562 cells, utilizing top-performing sgRNAs. All the screening results were validated through cytotoxicity assays (Fig. 1H).

To characterize the gene candidates, we performed Gene Ontology (GO) enrichment analysis and assessed the enrichment of sgRNAs that target genes involved in BTN family member interactions, type II interferon signaling, Kaposi sarcoma-associated herpesvirus infection, signal peptide processing and T-cell activation in the screened A375 cells (Fig. 2A). Among the screened K562 cells, Nef-mediated downregulation of CD4 expression, the RFX5-RFXANK-RFXAP complex, BTN family inter-actions, and iron uptake and transport were the most enriched biological pathways (Fig. 2B).

Overall, the screening experiments revealed a comprehensive picture of the pathways involved in pAg-dependent cytotoxicity. We found 11 overlapping genes from these screening experiments (BTN2A1, BTN3A1, BTN3A3, BTN3A2, SPCS3, ICAM1, DYRK1A, IFNGR2, HIST1H2BL, RFXAP, and QPCTL) (Fig. 2C). In addition, the clinical significance of the abundance of BTN3A2 and BTN3A3 for predicting the overall survival of melanoma patients was assessed via an analysis of a TCGA dataset (Fig. 2D). Because interactions between cell receptors and their ligands play important roles in the adhesion and activation of leukocytes, we expected to find some of these types of genes among the hits. Indeed, knocking out intercellular cell adhesion molecule-1 (ICAM-1) in A375 and K562 cells led to the evasion of T-cell killing (Fig. 1H). ICAM-1 is a cell surface glycoprotein and an adhesion receptor that regulates leukocyte recruitment and tethering in an LFA-1-dependent manner [19]. Our findings were consistent with those of previous studies in which blocking the ICAM-1/LFA-1 interaction resulted in attenuated activation of Vγ9Vδ2 T cells [20].

We further analyzed genetic determinants, and the corresponding deletion mutants in melanoma cells evaded NY-ESO-1 antigen-specific αβ T-cell killing [21]. This analysis revealed gene deletions that contribute to phenotypes associated with escape from αβ and Vγ9Vδ2 T-cell killing (Fig. 2E). Specifically, interferon gamma signaling molecules (IFNGR2, JAK2, and STAT1), cell death-related molecules (FADD, CASP8, and PMAIP1), and ICAM-1 were identified in both screening experiments. Key nodes (FAS, CASP8, and FADD) of the Fas-dependent apoptotic pathway were found to be clustered in Vγ9Vδ2 T-cell screens (Fig. 1E and Supplementary Fig. S1B). Given that A375 cells were Fas positive (Supplementary Fig. S1D), our results suggested that the Fas-FasL axis plays a key role in mediating cancer immune evasion. Indeed, FasL dose-dependently killed A375 cells (Supplementary Fig. S1E).

Given that αβ- and Vγ9Vδ2 TCRs interact with distinct molecules on cancer cells, we investigated patient survival based on the abundance of BTN molecules in clinical samples from mixed T-cell
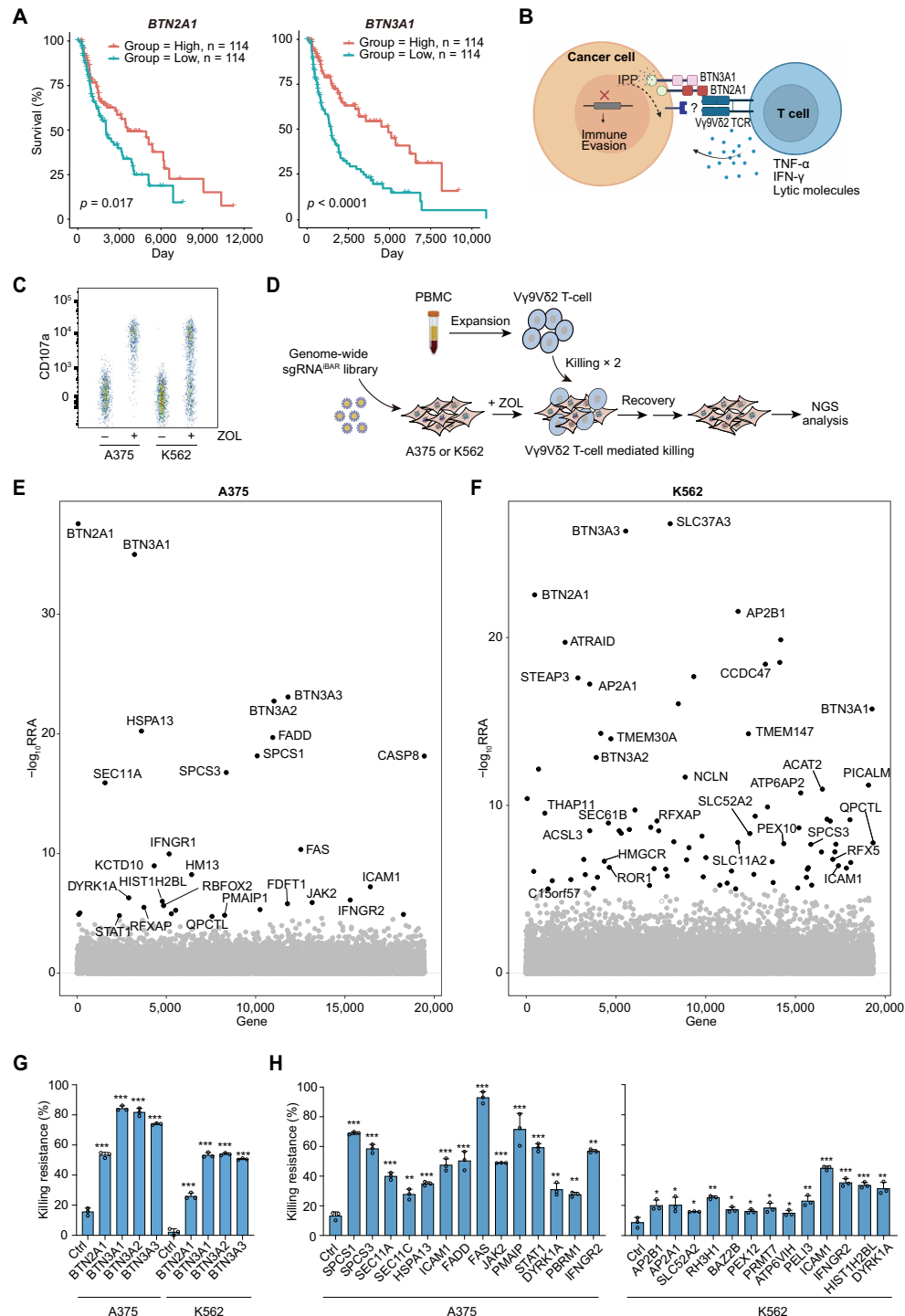
Fig. 1 Genome-wide CRISPR/Cas9 screening of A375 and K562 cells. **A** Kaplan–Meier curves showing differences in the overall survival of melanoma patients were stratified by the abundance of the BTN2A1 and BTN3A1 genes using The Cancer Genome Atlas dataset (OncoLnc). The 'High' and 'Low' groups were categorized according to the highest and lowest quartiles of individual gene expression, respectively. **B** Schematic of the current understanding of the activation of Vγ9Vδ2 T cells by cancer cells and an approach to identifying immune evasion genes. **C** Analysis of the degranulation of Vγ9Vδ2 T cells in response to cancer cells. **D** Workflow of whole-genome screening using two cell lines. A375/Cas9 or K562/Cas9 cells were infected with lentiviral sgRNAs and pretreated with ZOL overnight. Target cells were challenged twice with T cells. The reference cells were cultured and sequenced in parallel. **E** A375 cell screening hits. **F** K562 cell screening hits. The gene distributions were based on gene expression fold change values. **G** Killing resistance of two cell lines transduced with sgRNAs targeting BTN molecules or nontargeting control sgRNAs to expand Vγ9Vδ2 T cells. **H** A375 or K562 cell resistance to killing by expanded Vγ9Vδ2 T cells. Knockout or negative control cells (mCherry+) were cultured with control cells (GFP+mCherry+) in equal numbers and either treated with expanded Vγ9Vδ2 T cells or left untreated. The percentage of mCherry+ cells was measured by flow cytometry, and the degree of killing resistance was compared between the Vγ9Vδ2 T-cell-treated group and the untreated group. The data presented encompass three replicates using Vγ9Vδ2 T cells obtained from a donor, distinct from those employed in the CRISPR screens. The data are representative of two independent experiments using two human donors (**G** and **H**). The data are reported as the mean ± SD ($n = 3$). The horizontal lines indicate the means. *$p < 0.05$; **$p < 0.01$; ***$p < 0.001$. The Mann–Whitney U test was used
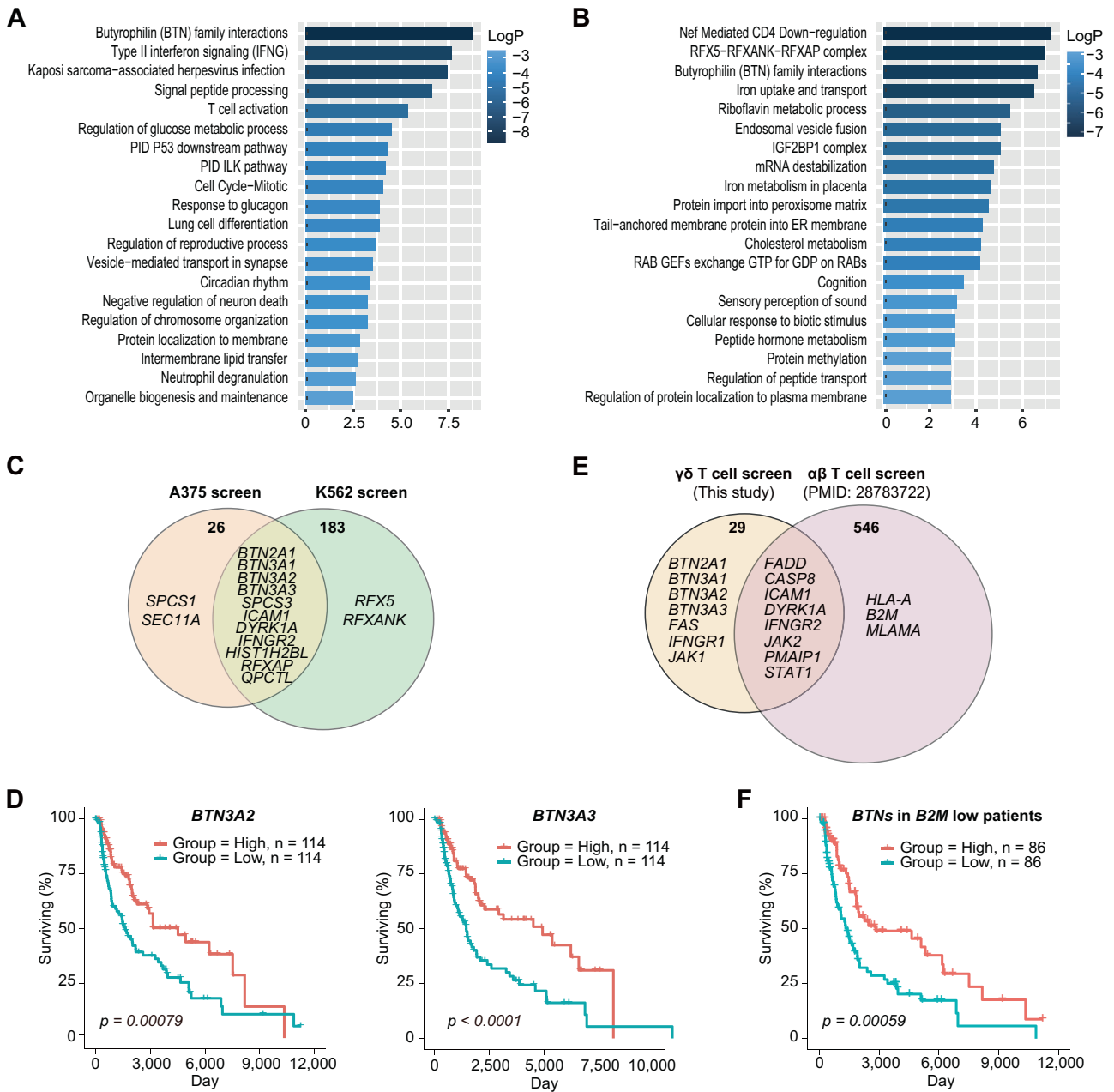
Fig. 2 Characterization of gene candidates from the two screening experiments. **A**, **B** GO enrichment analysis via Metascape. Enrichment analysis of enriched candidates in the A375 or K562 screening experiments (FDR < 0.2%). Pathways were ranked by an RRA score <1E−03. **C** Overlapping genes with an FDR < 0.2% across two cell lines (K562 and A375). **D** Kaplan–Meier curves showing differences in the overall survival of melanoma patients stratified by the abundance of the BTN3A2 and BTN3A3 genes using The Cancer Genome Atlas dataset (OncoLnc). The 'High' and 'Low' groups were categorized according to the highest and lowest quartiles, respectively, of the expression of each individual gene. **E** Common hits from melanoma cell screens using Vγ9Vδ2 T cells or NY-ESO-1 T cells. **F** Kaplan–Meier curves showing differences in the overall survival of melanoma patients stratified by the abundance of combined BTN molecules in low *B2M*-expressing samples. The 'High' and 'Low' groups were categorized according to the highest and lowest quartiles of combined BTN gene expression

populations. Notably, *B2M* is a well-established predictive marker of melanoma patient survival because of its universal role in supporting the expression of HLA and the recognition of the αβ T-cell TCR [21]. However, activation of Vγ9Vδ2 T cells by cancer cells is independent of the presence of B2m [22]. To determine whether the abundance of BTN molecules can predict the clinical outcome of patients with low B2M expression, we fractionated 75% of the samples and analyzed the associations between the abundance of the four BTN molecules and clinical outcomes. We observed that a reduction in the overall survival of these patients was associated with low expression of BTN molecules in tumors,

supporting the idea that αβ and Vγ9Vδ2 T cells exert a synergistic beneficial effect in inhibiting the growth of melanoma (Fig. 2F).

Transcriptionally synchronized BTN2A1/BTN3A1/BTN3A2/BTN3A3 expression was regulated by the RFX complex and IFN-γ signaling

Our screening experiments revealed a nonredundant role for each of the four BTN molecules in cancer cell killing by Vγ9Vδ2 T cells; however, the expression of these molecules among a range of cancer cells is unknown. In addition, whether these BTN molecules are coexpressed in cancer cells through a mechanism that drives

synergistic effects is unclear. Thus, we analyzed the expression of the four BTN transcripts in 1305 cell lines. This analysis revealed heterogeneous expression of these molecules across cancer cell lines (Fig. 3A). The coexpression pattern found in a few thousand cell lines suggested that BTN3A molecules are highly coexpressed with each other and, to a lesser extent, with BTN2A1 (Fig. 3A).

The coexpression of these two transcripts suggested that these molecules may be subjected to regulation by the same transcription factor(s). Our pathway analysis revealed that depletion of *RFX5*, *RFXAP*, or *RFXANK* in cancer cells led to evasion of Vγ9Vδ2 T-cell death (Fig. 2B). Regulatory factor X-5 (RFX5) is a winged-helix transcription factor (TF) that forms a heterotrimeric protein complex with RFXANK and RFXAP [23]. The RFX complex binds to a conserved DNA-binding domain and is involved in the regulation of HLA molecule expression [24, 25]. We reasoned that the RFX complex regulates the expression of BTN genes and noted that none of the TFs were clearly associated with the regulation of BTN molecule expression. We first analyzed the ChIP-seq data of RFX5 in K562 cells using ENDOTE (Fig. 3B). The results revealed specific binding of RFX5 to the X-box motif located in the promoter region of the BTN gene, which included the noncoding regions LOC285819 and BTN2A3P (Fig. 3B). To demonstrate the direct role of the RFX complex in regulating the abundance of BTN, we generated K562 cells lacking each component of the RFX complex. We found that RFX complex-knockout cells expressed lower levels of the BTN3A1/2/3 protein than did control cells (Fig. 3D). This finding aligns with the analysis of the total amount of BTN3A1 (Supplementary Fig. S2). Accordingly, *RFX5*-, *RFXAP*-, and *RFXANK*-knockout cells treated with ZOL or the anti-BTN3A antibody exhibited significant resistance to lysis by Vγ9Vδ2 T cells (Fig. 3E and Supplementary Fig. S3).

Our screening experiments further suggested that knocking out genes in the IFN-γ signaling cluster (*IFNGR1*, *IFNGR2*, *STAT1*, *JAK1* and *JAK2*) resulted in resistance to Vγ9Vδ2 T-cell killing (Fig. 1F). As IFN-γ treatment enhances RFX complex activity and increases the expression of HLA molecules [24], we hypothesized that BTN molecules are subjected to similar transcriptional regulation. NLRC5 has been implicated in the transcriptional regulation of the MHC and BTN genes [26]. Upon IFN-γ treatment, phosphorylated STAT1 promoted the expression of NLRC5. Subsequently, the NLRC5 and RFX complexes bound to specific DNA domains and upregulated the expression of BTN genes (Fig. 3F). The increase in the surface abundance of BTN3As was confirmed by IFN-γ treatment (Fig. 3G). Together, our results support the idea that the transcriptional synchronization of BTN molecules mediated by IFN-γ signaling and the RFX5 complex is essential for priming TCR interactions and mounting robust immune responses.

Posttranslational synchronization involving pyroglutamate modification of BTN molecules is integral to the recognition and killing of target cells by Vγ9Vδ2 T cells
Because nothing is known about posttranslational modifications to BTN proteins, we first analyzed the sequence and structure of the four BTN proteins. We noted that N-terminal glutamine (Gln) is a common feature of BTN sequences (Fig. 4A). The position of glutamine is highlighted in the extracellular IgV domain of the BTN protein (Fig. 4B). These glutamines can potentially be subjected to pyroglutamate modification. Our screening results suggested that knocking out *QPCTL* in cancer cells promoted evasion of Vγ9Vδ2 T-cell killing (Fig. 2C). *QPCTL* encodes glutaminyl-peptide cyclotransferase-like (QPCTL), a protein that catalyzes the formation of pyroglutamate residues (pyro-Glu) through cyclization of N-terminal glutamine and glutamate residues [27]. We hypothesized that BTNs are QPCTL substrates and are thus subject to pyroglutamate modification. To provide evidence of the pyroglutamate modification of BTN proteins, we developed a mass spectrometry-based assay and confirmed the

pyroglutamate modification of BTN2A1, BTN3A2, and BTN3A3 (Fig. 4C and Supplementary Fig. S4).

After confirming that QPCTL deletion in cancer cells resulted in significant resistance to killing by Vγ9Vδ2 T cells (Figs. 4D and Supplementary Fig. S5), we proceeded to examine whether QPCTL contributes to the recognition of cancer cells by Vγ9Vδ2 T cells. We performed a short-term cell conjugation assay and observed impaired cell conjugation between Vγ9Vδ2 T cells and QPCTL-deficient cancer cells (Fig. 4E). Given that the BTN molecule interacts with Vγ9Vδ2 TCRs, we hypothesized that pyroglutamate modification of BTN molecules is critical for these interactions. We evaluated the binding of TCR tetramers to K562 cells and found that TCR binding was abolished in QPCTL knockout (KO) cells, suggesting that QPCTL is critical for TCR tetramer staining (Fig. 4F). We further applied the glutaminyl cyclase inhibitor SEN177 to inhibit the enzymatic activity of QPCTL [28]. SEN177-treated cancer cells exhibited resistance to Vγ9Vδ2 T-cell killing, suggesting that QPCTL has an enzymatic contribution to the evasion of Vγ9Vδ2 T-cell cytotoxicity (Fig. 4G).

We next evaluated the abundance of BTN3A molecules in QPCTL-deficient cells. Diminished cell surface staining of BTN3A, but not all BTN3A proteins, was detected in QPCTL-deficient cells (Fig. 4H). We did not find an antibody against cell surface BTN2A1 but found that the total amount of BTN2A1 was unaltered in these cells (Supplementary Fig. S6A). This result was very similar to the observation of CD47 abundance in QPCTL-knockout cells. As previously shown, QPCTL is critical for pyroglutamate modification of CD47 at the SIRPα-binding site [28]. To demonstrate the critical role of N-terminal pyro-Glu in BTN3A1 detection, wild-type BTN3A1 or N-terminal glutamine-mutated BTN3A1 (Q30R) was overexpressed in HEK293T cells. The cells transfected with mutant BTN3A1 had substantially lower BTN3A1 staining intensity on the cell surface than the cells transfected with the wild-type control; however, the total amount of the BTN3A1 protein was unaltered (Fig. 4I). Additionally, the total amount of the BTN2A1 protein was similar in cells transfected with either the wild-type or N-terminal glutamine mutated plasmid (Q30R) (Supplementary Fig. S6B). Together, our results suggest that QPCTL is a critical enzymatic effector of BTN proteins; therefore, a lack of QPCTL expression causes defective pyroglutamate modification of BTN molecules and leads to the evasion of Vγ9Vδ2 T-cell killing (Fig. 4J).

The TMCO1 translocon complex is involved in the accumulation of phosphoantigens and in the activation of Vγ9Vδ2 T cells
Clinically, ZOL is emerging as an essential small molecule in cancer therapy that interacts with Vγ9Vδ2 T cells. The anticancer effect of expanded Vγ9Vδ2 T cells combined with ZOL administration has been demonstrated in a clinical trial [13]. Additionally, a ZOL-conjugated therapeutic antibody has been developed to specifically target cancer cells [14]. Bisphosphonate drugs are hydrophilic molecules that cannot cross cellular membranes through passive diffusion. Cellular uptake of bisphosphonate drugs requires fluid-phase endocytosis. In addition, membrane transport proteins are required to release drugs from endocytic vesicles into the cytosol [29]. Through our screening, the deletion of genes that are important for this uptake and release process impaired the accumulation of intracellular IPP and the activation of T cells. Indeed, the top ranked gene in the K562 cell screening was *SLC37A3* (Fig. 1F), which mediates the release of bisphosphonate molecules from acidic endosomes into the cytosol in cancer cells [30]. We did not identify these genes in the A375 cell screening. These differences might be related to the efficiency of ZOL processing in different cells and to cell susceptibility to Vγ9Vδ2 T-cell killing.

Our results highlighted a newly identified ribosome translocon complex and provided evidence about its role in the evasion of ZOL-directed Vγ9Vδ2 T-cell cytotoxicity. The complex contains the core Sec61 channel and five accessory factors, TMCO1, CCDC47,

Fig. 3 The RFX complex upregulates the expression of BTN molecules. **A** The coexpression of paired BTN mRNA molecules across cancer cell lines. **B** Genomic tracks of mapped ChIP-seq reads at BTN loci. **C** Alignment of the DNA binding sequence of the RFX complex. The binding region was exemplified at the BTN3A2 locus. **D** Flow cytometry analysis of BTN3A1/2/3 cell surface abundance on K562 cells. Knockout cells were compared to negative control cells. The staining controls are indicated as dashed lines. **E** Killing of K562 cells transduced with sgRNAs targeting the indicated genes or nontargeting control sgRNA. **F** Schematic graph of the transcriptional regulation of BTN genes. IFN-γ induces NLRC5 expression through STAT1 activation. NLRC5 forms a protein complex with RFX/RFXAP/RFXANK, and these components collaboratively promote the expression of BTN molecules. **G** Cell surface abundance of BTN3A1/2/3 on K562 cells with or without IFN-γ treatment. The staining controls are indicated as dashed lines. The results are representative of three independent experiments (**D**, **E**, **G**). The data are reported as the mean ± SD in E ($n = 3$). The horizontal lines indicate the means. ***$p < 0.001$. The Mann–Whitney U test was performed
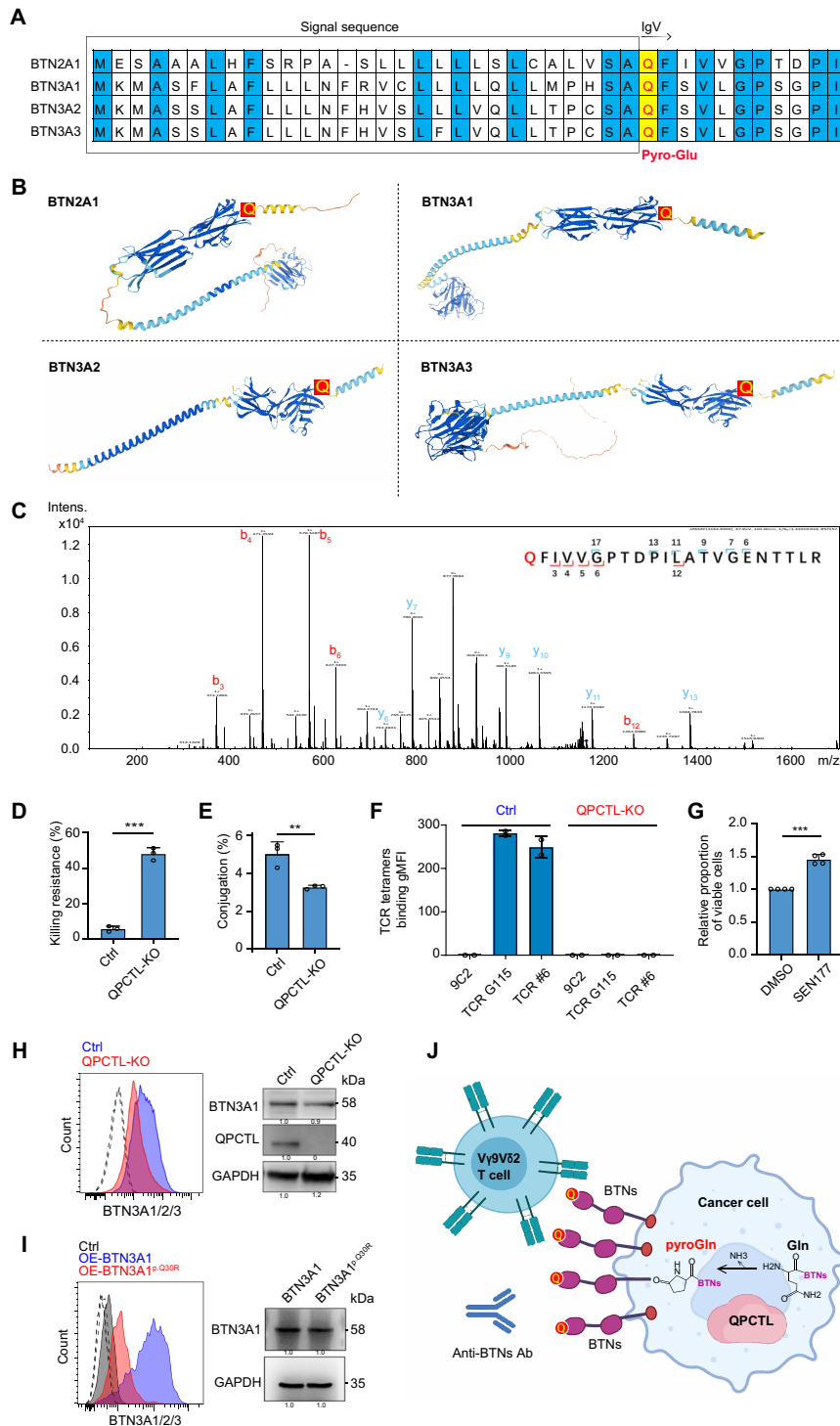
Fig. 4 Pyroglutamate modification of BTN molecules contributes to the elimination of cancer cells by Vγ9Vδ2 T cells. **A** Schematic of the primary sequence of BTN molecules. The signal peptide sequences are indicated by the box. **B** Structures of four BTN molecules were predicted by AlphaFold. The N-terminal glutamine residues are highlighted in red. **C** MS/MS spectrum of the identified pyroglutamyl peptide of BTN2A1. The characteristic b and y ions are annotated on the sequence in red and blue, respectively. **D** Killing of K562 cells transduced with sgRNAs targeting *QPCTL* or nontargeting control sgRNA by expanded Vγ9Vδ2 T cells. **E** Flow cytometry analysis of the conjugation of Vγ9Vδ2 T cells and K562 cells transduced with sgRNAs targeting *QPCTL* or nontargeting sgRNA. **F** TCR tetramer expression in two types of K562 cells was measured after overnight ZOL treatment. The intensity of tetramer staining was used to calculate TCR binding before and after ZOL treatment. The Vγ5Vδ1[+] TCR (9C2) served as a negative control. **G** Killing of A375 cells treated with either DMSO or SEN177 by expanded Vγ9Vδ2 T cells. **H** The surface expression of BTN3A1/2/3 on K562 cells transduced with sgRNAs targeting *QPCTL* (red) or nontargeting control sgRNA (blue). The staining controls are indicated as dashed lines. Two types of K562 cells were lysed and blotted with antibodies recognizing the indicated antigens. **I** The surface abundance of BTN3A1/2/3 on HEK293T cells transfected with wild-type BTN3A1 (blue) or mutated BTN3A1 (red). Native BTN3A expression in HEK293T cells is indicated in gray. HEK293T cells overexpressing BTN3A1 or mutated BTN3A1 were lysed and blotted with anti-BTN3A1. **J** Schematic graph of the contribution of QPCTL to the pyroglutamate modification of BTN molecules. The data are representative of two experiments. The data are reported as the mean ± SD in **D**–**G** ($n = 3$). **$p < 0.01$; ***$p < 0.001$. The Mann–Whitney U test was performed

Nicalin, TMEM147 and NOMO, and contributes to the biogenesis of multipass membrane proteins [31]. Notably, *CCDC47*, *TMEM147*, *NCLN* (encoding Nicalin), *SEC61B*, and *TMCO1* were clustered in our screening experiment (Fig. 5A, B). The ribosome translocon complex is critical for protein biogenesis, including protein folding, topogenesis, and chemical modification. We reasoned that this complex may be involved in the regulation of protein biogenesis by either BTNs or cellular mediators involved in the

uptake and release of ZOL. To identify mRNA targets of the TMCO1 translocon complex, we analyzed the mRNAs associated with ribosomes that had been recovered by affinity purification of TMCO1 (GSE134027). This analysis revealed 22 hits in the K562 cell screening, and their gene products, which included *SLC37A3*, *STEAP3*, *SLC52A2*, *SLC11A2*, *SLC30A6*, and *SLC52A2*, were targets of the TMCO1 translocon complex (Fig. 5C, D). Consistent with the role of the TMCO1 translocon complex in the biogenesis of
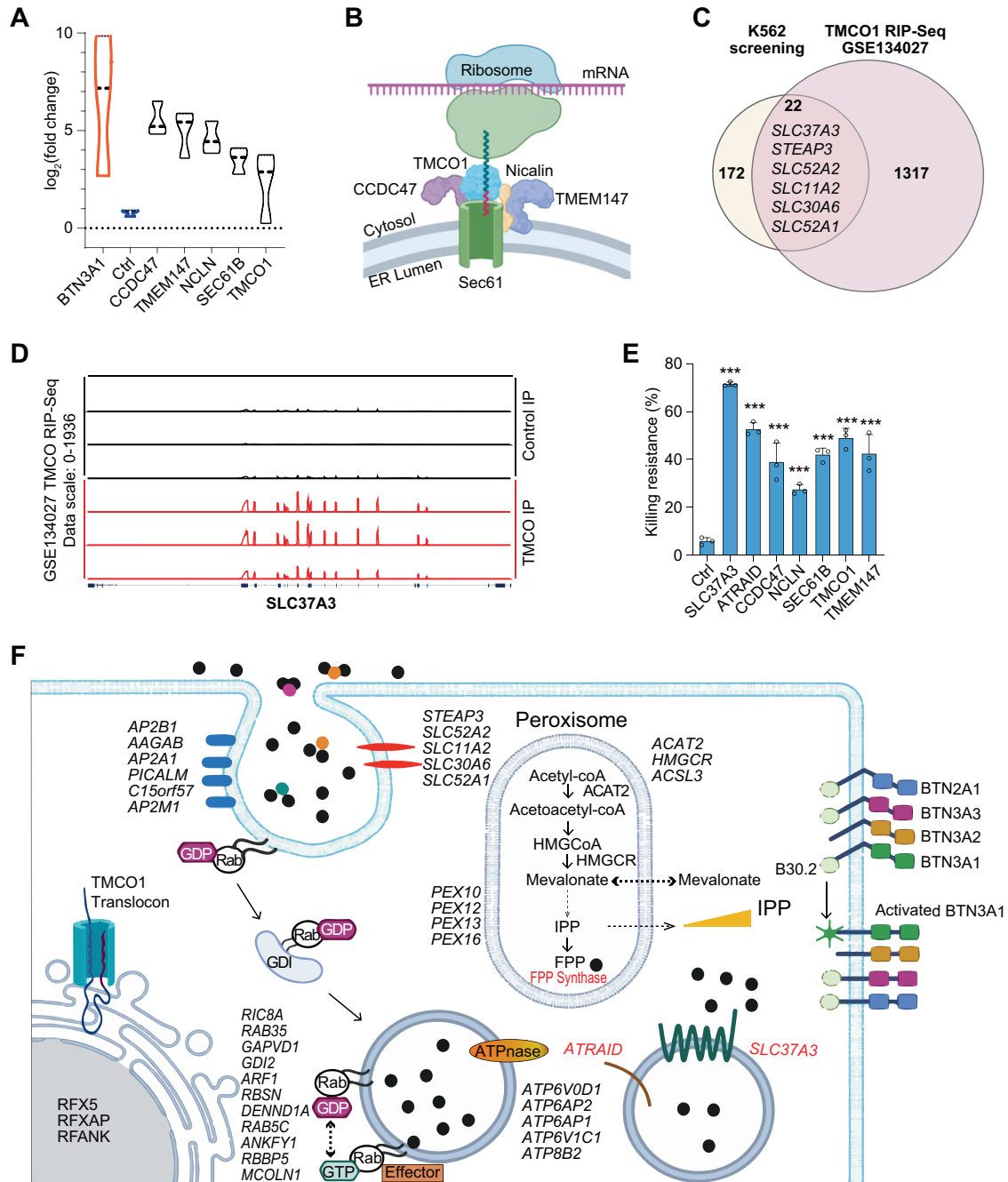

Fig. 5 The top-ranked genes from the K562 screen are involved in the cellular processing of ZOL. **A** SgRNA-level analysis showing the differential fold change (FC) distributions of sgRNA targeting the TMCO1 complex from the K562 screening. BTN3A1 was used as the positive control. **B** Cartoon depicting the TMCO1 complex from a previous study (NOMO was not depicted). **C** Overlapping gene hits of the K562 screen and mRNAs associated with ribosomes recovered after affinity purification of TMCO1. **D** Genomic tracks of mapped TMCO1 RNA immunoprecipitation sequencing reads at the *SLC37A3* locus. **E** Killing of K562 cells transduced with sgRNAs targeting the indicated genes or nontargeting control sgRNA by expanded Vγ9Vδ2 T cells. **F** Schematic of ZOL entry, transport, and release using the top-ranked hits from the K562 screening. The data are reported as the mean ± SD in E ($n = 3$). The horizontal lines indicate the means. The data are representative of two experiments using two donors. ***$p < 0.001$. The Mann–Whitney U test was performed

multipass membrane proteins, the mRNAs of BTN molecules were not detected (Supplementary Fig. S7). This finding suggested that the biogenesis of multipass membrane proteins involved in the cellular processing of ZOL, such as SLC37A3, is impaired by perturbations of the TMCO1 translocon complex. We confirmed that deletion of the SLC37A3/ATRAID complex and TMCO1 translocon complex components resulted in substantial resistance to lysis by Vγ9Vδ2 T cells (Fig. 5E).

In addition, sgRNAs targeting multiple regulators of clathrin-mediated endocytosis, including members of the heterotetrameric adaptor protein complex-2 (AP-2), phosphatidylinositol-binding clathrin assembly protein (encoded by PICALM), and the newly identified C15orf57 [32], were enriched in surviving K562 cells. Multiple iron receptors, such as STEAP3, SLC52A2, SLC11A2, SLC30A6, and SLC52A1, were identified as strong hits (Fig. 1F). Given that BPs are chelators of iron, iron/ZOL complexes likely facilitate the uptake of ZOL. The deletion of key enzymes in the mevalonate pathway cascade results in reduced production of IPP in cancer cells [33]. Along these lines, ACAT2, HMGCR, and ACSL3 were identified in our screen. The presqualene segment of the cholesterol biosynthetic pathway is localized in peroxisomes, and the reactions between mevalonate and farnesyl diphosphate are assumed to be exclusively peroxisomal [34]. Our results suggest that a set of genes encoding peroxisomal machinery components (PEX10, PEM12, PEM13, and PEM16) may be involved in the transportation of ZOL into peroxisomes. We summarized these findings in a schematic diagram on the basis of pathway enrichment analysis and the analysis of existing data and the literature (Fig. 5F). Collectively, these findings expand the knowledge of the cellular regulators contributing to IPP accumulation in response to ZOL treatment.

DISCUSSION
Mapping genetic determinants of cancer cell immune evasion informs efforts to promote cancer immunotherapy strategies. By performing screening with functionally and genetically diverse cell lines, our study provides a reference set of genes and pathways that mediate intrinsic Vγ9Vδ2 T-cell cancer cell evasion.

Overexpression of the BTN3A1 and BTN2A1 molecules in rodent cells is sufficient to activate Vγ9Vδ2 TCR-expressing cells [5, 6, 35]. Although this approach is valuable for investigating protein interactions, experimental target cells are not representative of the physiological abundance of BTN molecules in cancers, and such a predisposed approach may lead to the oversight of meaningful molecule(s) involved in the immune response. For example, BTN plasmid transfection resulted in a high abundance of BTN antigens on the cell surface compared with those on native control cells (Supplementary Fig. S8) [17].

Our screening experiments established the categorical role of four BTN molecules in untransfected cancer cells that evade primary Vγ9Vδ2 T-cell killing. The roles of BTN3A1 in sensing pAgs and activating Vγ9Vδ2 T cells have been extensively studied, including the structural and functional aspects of its juxtamembrane region and B30.2 domain [10, 36–40]. Additionally, BTN3A1 has been shown to inhibit the activation of tumor-reactive αβ T cells by preventing segregation of N-glycosylated CD45 from the immune synapse [41]. This inhibitory effect of BTN3A1 on αβ T cells is unlikely to be applicable to Vγ9Vδ2 T cells since the knockout of BTN3A1 in cancer cells is expected to promote the activation of Vγ9Vδ2 T cells. In contrast, the ability of BTN3A2 and BTN3A3 in cancer cells to activate Vγ9Vδ2 T cells has been inconsistent across multiple studies [35, 42, 43], which may be related to differences in the experimental settings. One study demonstrated that BTN3A2 regulates the subcellular trafficking and stability of BTN3A1, thereby contributing to the activation of Vγ9Vδ2 T cells [35]. We hypothesized that BTN3A2 and BTN3A3 'catalyze' the interactions between Vγ9Vδ2 TCR and its ligand(s) and are critical for the initiation of robust immune responses via several mechanisms that work individually or in concert. The role of BTN3A2 and BTN3A3 in Vγ9Vδ2 T-cell activation has been described in studies using agonist antibodies [17, 42]. Agonist stimulation is thought to mimic pAg-mediated signaling by cross-linking BTN3A molecules. The extracellular domain of each individual BTN3A molecule is capable of activating Vγ9Vδ2 T cells via agonist antibody stimulation in the presence of BTN2A1 [17, 42]. This is particularly pertinent to a genetic analysis showing extreme homogenization of the extracellular IgV sequences of BTN3A molecules, thereby suggesting the presence of an evolutionarily conserved functional domain in BTN3A molecules [44].

BTN3As are crucial molecules for the anticancer activity of Vγ9Vδ2 T cells, but the cellular receptor(s) of these proteins have yet to be identified. Therapeutic antibodies targeting BTN3A have been developed to activate Vγ9Vδ2 T cells for clinical application [17, 45, 46]. This approach is based on the observation that crosslinking BTN3A proteins on the surface of cancer cells with anti-BTN3A antibodies results in the activation of Vγ9Vδ2 T cells. Notably, QPCTL is a key checkpoint of Vγ9Vδ2 T-cell activity that posttranslationally synchronizes N-terminal glutamine residues in IgV sequences of BTN3A molecules. We demonstrated that pyroglutamate modification of BTN3As mediated by QPCTL is critical for the detection of anti-BTN3A antibodies, which is relevant to therapeutic antibodies based on Vγ9Vδ2 T-cell biology [47, 48].

In a recent study, CRISPR screens were employed to investigate the metabolic pathways that regulate the abundance of BTN3A on the cell surface [49]. In contrast, our study specifically examined the transcriptional, posttranscriptional, and functional synchronization of BTN molecules. These findings offer distinct insights into the regulatory and functional significance of BTN molecules in the context of γδ T-cell-mediated tumor immunity. Clinically, ZOL is emerging as an essential small molecule in cancer therapy that interacts with Vγ9Vδ2 T cells. The anticancer effect of expanded Vγ9Vδ2 T cells combined with ZOL administration has been demonstrated in a clinical trial [13]. Additionally, ZOL-conjugated therapeutic antibodies have been developed to target cancers by utilizing Vγ9Vδ2 T cells [14]. Therefore, identifying the cellular factors involved in ZOL processing in the context of Vγ9Vδ2 T-cell biology is meaningful. Together with other characterized genetic components and circuits that regulate cancer cell responses to Vγ9Vδ2 T cells, our genome-wide functional study provides important groundwork for future genotype-driven applications of Vγ9Vδ2 T-cell immunotherapies.

METHODS
Cells
Peripheral blood mononuclear cells (PBMCs) were collected from deidentified healthy donor pheresis products. K562 cells were maintained in RPMI 1640 medium (Gibco). A375 cells were cultured in Dulbecco's modified Eagle's medium (Gibco). All media contained 10% fetal bovine serum (FBS; Biological Industries) and were supplemented with penicillin and streptomycin (Gibco). All cells were routinely checked for mycoplasma contamination. Vγ9Vδ2 T cells were expanded with 5 μM zoledronic acid (DengMiBio) and 100 IU/ml interleukin-2 (IL-2; Sihuan ShengWu). The purity of the Vγ9Vδ2 T cells was evaluated on day 9 post expansion.

Mice
The nude mice (6 to 8 weeks old) were obtained from Beijing Vital River Laboratory Animal Technology Co., Ltd. All the mice were kept under specific pathogen-free conditions in the Laboratory Animal Center of Peking University. All animal work was approved by the Institutional Animal Care and Use Committee at Peking University. A total of 15 million color barcoded mCherry-expressing K562 cells and Vγ9Vδ2 T cells were simultaneously injected into the peritoneal cavity of mice, thereby maintaining the effector-to-target (E:T) ratio of 2. After a 24-h period, peritoneal lavage fluid was collected by washing with cold PBS.

Lentiviral production and infection
To produce the lentivirus, HEK293T cells were transfected with a lentiviral transfer vector, the packaging plasmid pR8.74 (#22036; Addgene), and

VSVg (#158233; Addgene) using X-tremeGENE HP DNA Transfection Reagent (Roche). The sgRNA-transduced cells were then treated with culture medium containing puromycin (5 µg/ml for K562 cells and 1 µg/ml for A375 cells) to select for the transduced cells.

Genome-wide CRISPR screen and functional enrichment analysis

The screening experiments using the CRISPR sgRNA[iBAR] library were conducted as previously described [18]. Cas9-expressing K562 and A375 cells were infected with a pooled lentiviral genome-wide sgRNA library at a multiplicity of infection of three and selected with puromycin after seventy-two hours of infection. The cells were maintained at a minimum coverage of 1000x for two rounds of killing experiments. For the experimental group, K562 cells were pretreated with 12.5 µM ZOL for 12 h, and A375 cells were pretreated with 6.25 µM ZOL for 12 h. For the K562 cell screening experiments, Vγ9Vδ2 T cells were added at an E:T ratio = 1:2 in the first round of killing and an E:T ratio = 1:1 for the second round of killing. A375 cell screening experiments were performed at incremental E:T ratios. The cells resistant to Vγ9Vδ2 T-cell killing were expanded for an additional 7 days between the two rounds of T-cell treatment. Genomic DNA was extracted with DNeasy Blood & Tissue Kits (QIAGEN), and next-generation sequencing (NGS) was performed by GENEWIZ. The MAGeCK[iBAR] analysis pipeline was used to calculate the positive screening scores of all the targeted genes [18]. We used Metascape (https://Metascape.org/) to perform Gene Ontology (GO) analysis. Gene annotations were retrieved from the UCSC hg38 genome, which contains 19,210 genes. For each gene, three different sgRNAs with four barcodes were designed using our newly developed DeepRank algorithm. An additional 1000 nontargeting sgRNAs, each with four barcodes, served as negative controls.

BTN molecule coexpression analysis and survival analysis

The RNA-seq data of 1305 cancer cell lines were obtained from the Cancer Cell Line Encyclopedia (CCLE) database, and the Pearson correlation between corresponding gene pairs was calculated. The clinical outcome of melanoma patients from the TCGA dataset was analyzed using OncoLnc (http://www.oncolnc.org/).

Flow cytometry reagents and analysis

The following antibodies and cytokines obtained from BioLegend were used for flow cytometry: anti-CD3e (UCHT1), anti-CD107a (H4A3), anti-CD56 (HCD56), anti-TCRVδ2 (B6), anti-HLA-ABC (W6/32), anti-TCRVγ9 (B3) and recombinant human FASL. An anti-CD277 (BT3.1) antibody was obtained from Novus Biologicals. An anti-Fas (REA738) antibody was obtained from Miltenyi Biotec. Vγ5Vδ1 TCR (clone 9C2) and Vγ9Vδ2 TCR (clone G115 and TCR6) tetramers were generated as previously described [4]. To activate tumor cells utilizing the anti-BTN3A antibody (eBioBT3.1; Invitrogen), K562 cells were incubated with the antibodies for 2 h at a concentration of 10 µg/ml. Subsequently, the cells were washed and cultured with Vγ9Vδ2 T cells. For the CD107a assay, ZOL-treated K562 and A375 cells were coincubated with Vγ9Vδ2 T cells for 4 h in the presence of an anti-CD107a antibody to detect degranulation. DAPI (BioLegend) was applied to exclude dead cells. To upregulate BTN expression, human IFN-γ (BioLegend) was added at a concentration of 1000 IU/ml, and the mixture was incubated for 24 h. Flow cytometry was performed with a Fortessa flow cytometer (BD Biosciences).

Competitive killing assay

Knockout (mCherry^{+}) cells and control cells (GFP[+]mCherry[+]) were mixed at a ratio of 1:1 and seeded in 96-well plates. The target cells were then treated with ZOL for 12 h and washed twice in media before Vγ9Vδ2 T cells were added (E:T ratio = 1:4). After 16 h, the percentage of GFP^{+} cells was measured by flow cytometry, while CD3 and DAPI staining were used to exclude T cells and dead cells, respectively. Killing resistance was calculated based on the ratios of the Vγ9Vδ2 T-cell-treated and untreated groups, and the percentage of killing resistance was calculated using the following formula: % killing resistance = 100*(1-(P2/(100-P2)*(100-P1)/P1)); where P1 = % of the target cells in the group without effector cells (i.e., % of GFP^{+} cells); and P2 = % of the target cells in the group with T cells (% of GFP^{+} cells).

Cell conjugation assay

Control K562 cells were labeled with 2.5 µM CFSE (BioLegend), and QPCTL-knockout K562 cells were labeled with 2.5 µM CTV (Invitrogen). The labeled target cells were cultured overnight before the T cells were added. Equal amounts of target cells and Vγ9Vδ2 T cells were added to 96 V plates and spun at 500 rpm for 1 min. The plate was incubated in a 37 °C water bath for 5 min and immediately fixed by adding 50 µl of ice-cold paraformaldehyde buffer. The cells were pipetted 5 times and transferred to FACS tubes for cell conjugation analysis.

Absolute counting of viable cells

A375 cells were treated with 10 µM SEN-177 (SML1615; Sigma Aldrich) or DMSO for 48 h. The cells were treated with 6.25 µM ZOL for 16 h. After extensive washing, Vγ9Vδ2 T cells were added to the culture at an E:T ratio of 1:4 for 16 h. A375 cells were detached, and live cells were detected via Annexin-V (Procell) and DAPI staining. Absolute counting beads (BioLegend) were used to determine the absolute number of viable cells.

Western blotting and immunoprecipitation

HEK293T cells were transfected with BTN- or BTN-carrying p.Q30R plasmids. After 2 days, the cell pellets were collected, and radio-immunoprecipitation assay buffer was used to lyse the cells on ice for 15 min with protease inhibitors. The lysed cells were then denatured via the addition of Laemmli sample buffer and heated before processing for western blotting detection. The following antibodies were used: anti-BTN2A1 (NBP2-92020; Novus Biologicals), anti-BTN3A1 (ab236289; Abcam), and anti-QPCTL (Santa Cruz Biotechnology). For immunoprecipitation, HEK293T cells were transfected with BTN-Flag plasmids, and cell lysates were incubated with an anti-FLAG M2 affinity gel (A2220, Sigma–Aldrich). After gel separation, the samples were lysed and analyzed by liquid chromatography-tandem mass spectrometry (LC–MS/MS). Briefly, the cell powder was then transferred to a centrifuge tube, and four volumes of lysis buffer were added. Sonication was performed on ice for 3 min using a high-intensity ultrasonic processor. The protein concentration was determined using a BCA kit. The tryptic peptides were dissolved in solvent A and loaded onto a custom-made reversed-phase analytical column. A gradient of solvent A and solvent B was used to separate the peptides, and the eluted peptides were analyzed using a timsTOF Pro 2 mass spectrometer. The resulting MS/MS data were processed using the MaxQuant search engine.

Statistical analysis

The Mann–Whitney U test was performed to compare the ratios between two groups. The results were considered to be significant when the two-sided P value was 0.05. *$P < 0.05$; **$P < 0.01$; ***$P < 0.001$.

DATA AVAILABILITY

All the data needed to evaluate the conclusions in the paper are presented in the paper or the supplementary materials.

REFERENCES

1. Constant P, Davodeau F, Peyrat MA, Poquet Y, Puzo G, Bonneville M, et al. Stimulation of human gamma delta T cells by nonpeptidic mycobacterial ligands. Science. 1994;264:267–70. https://doi.org/10.1126/science.8146660.
2. Xu Y, Xiang Z, Alnaggar M, Kouakanou L, Li J, He J, et al. Allogeneic Vγ9Vδ2 T-cell immunotherapy exhibits promising clinical safety and prolongs the survival of patients with late-stage lung or liver cancer. Cell Mol Immunol. 2021;18:427–39. https://doi.org/10.1038/s41423-020-0515-7.
3. Rhodes DA, Reith W, Trowsdale J. Regulation of Immunity by Butyrophilins. Annu Rev Immunol. 2016;34:151–72. https://doi.org/10.1146/annurev-immunol-041015-055435.
4. Rigau M, Ostrouska S, Fulford TS, Johnson DN, Woods K, Ruan Z, et al. Butyrophilin 2A1 is essential for phosphoantigen reactivity by gammadelta T cells. Science. 2020;367:eaay5516 https://doi.org/10.1126/science.aay5516.
5. Karunakaran MM, Willcox CR, Salim M, Paletta D, Fichtner AS, Noll A, et al. Butyrophilin-2A1 Directly Binds Germline-Encoded Regions of the Vgamma9Vdelta2 TCR and Is Essential for Phosphoantigen Sensing. Immunity. 2020;52:487–498 e486. https://doi.org/10.1016/j.immuni.2020.02.014.
6. Cano CE, Pasero C, De Gassart A, Kerneur C, Gabriac M, Fullana M, et al. BTN2A1, an immune checkpoint targeting Vgamma9Vdelta2 T cell cytotoxicity against malignant cells. Cell Rep. 2021;36:109359 https://doi.org/10.1016/j.celrep.2021.109359.
7. Vyborova A, Beringer DX, Fasci D, Karaiskaki F, van Diest E, Kramer L, et al. gamma9delta2T cell diversity and the receptor interface with tumor cells. J Clin Invest. 2020;130:4637–51. https://doi.org/10.1172/JCI132489.

8. Willcox CR, Vantourout P, Salim M, Zlatareva I, Melandri D, Zanardo L, et al. Butyrophilin-like 3 Directly Binds a Human Vgamma4(+) T Cell Receptor Using a Modality Distinct from Clonally-Restricted Antigen. Immunity. 2019;51:813–825 e814. https://doi.org/10.1016/j.immuni.2019.09.006.

9. Herrmann T, Karunakaran MM, Fichtner AS. A glance over the fence: Using phylogeny and species comparison for a better understanding of antigen recognition by human gammadelta T-cells. Immunol Rev. 2020;298:218–36. https://doi.org/10.1111/imr.12919.

10. Sandstrom A, Peigne CM, Leger A, Crooks JE, Konczak F, Gesnel MC, et al. The intracellular B30.2 domain of butyrophilin 3A1 binds phosphoantigens to mediate activation of human Vgamma9Vdelta2 T cells. Immunity. 2014;40:490–500. https://doi.org/10.1016/j.immuni.2014.03.003.

11. Hsiao CC, Nguyen K, Jin Y, Vinogradova O, Wiemer AJ. Ligand-induced interactions between butyrophilin 2A1 and 3A1 internal domains in the HMBPP receptor complex. Cell Chem Biol. 2022;29:985–995.e985. https://doi.org/10.1016/j.chembiol.2022.01.004.

12. Laplagne C, Meddour S, Figarol S, Michelas M, Calvayrac O, Favre G, et al. Vgamma9Vdelta2 T Cells Activation Through Phosphoantigens Can Be Impaired by a RHOB Rerouting in Lung Cancer. Front Immunol. 2020;11:1396 https://doi.org/10.3389/fimmu.2020.01396.

13. Wada I, Matsushita H, Noji S, Mori K, Yamashita H, Nomura S, et al. Intraperitoneal injection of in vitro expanded Vgamma9Vdelta2 T cells together with zoledronate for the treatment of malignant ascites due to gastric cancer. Cancer Med. 2014;3:362–75. https://doi.org/10.1002/cam4.196.

14. Benelli R, Costa D, Salvini L, Tardito S, Tosetti F, Villa F, et al. Targeting of colorectal cancer organoids with zoledronic acid conjugated to the anti-EGFR antibody cetuximab. J Immunother Cancer. 2022;10:e005660 https://doi.org/10.1136/jitc-2022-005660.

15. Ravens S, Schultze-Florey C, Raha S, Sandrock I, Drenker M, Oberdorfer L, et al. Human gammadelta T cells are quickly reconstituted after stem-cell transplantation and show adaptive clonal expansion in response to viral infection. Nat Immunol. 2017;18:393–401. https://doi.org/10.1038/ni.3686.

16. Gentles AJ, Newman AM, Liu CL, Bratman SV, Feng W, Kim D, et al. The prognostic landscape of genes and infiltrating immune cells across human cancers. Nat Med. 2015;21:938–45. https://doi.org/10.1038/nm.3909.

17. De Gassart A, Le KS, Brune P, Agaugue S, Sims J, Goubard A, et al. Development of ICT01, a first-in-class, anti-BTN3A antibody for activating Vgamma9Vdelta2 T cell-mediated antitumor immune response. Sci Transl Med. 2021;13:eabj0835 https://doi.org/10.1126/scitranslmed.abj0835.

18. Zhu S, Cao Z, Liu Z, He Y, Wang Y, Yuan P, et al. Guide RNAs with embedded barcodes boost CRISPR-pooled screens. Genome Biol. 2019;20:20 https://doi.org/10.1186/s13059-019-1628-0.

19. Bui TM, Wiesolek HL, Sumagin R. ICAM-1: A master regulator of cellular responses in inflammation, injury resolution, and tumorigenesis. J Leukoc Biol. 2020;108:787–99. https://doi.org/10.1002/jlb.2mr0220-549r.

20. Uchida R, Ashihara E, Sato K, Kimura S, Kuroda J, Takeuchi M, et al. Gamma delta T cells kill myeloma cells by sensing mevalonate metabolites and ICAM-1 molecules on cell surface. Biochem Biophys Res Commun. 2007;354:613–8. https://doi.org/10.1016/j.bbrc.2007.01.031.

21. Patel SJ, Sanjana NE, Kishton RJ, Eidizadeh A, Vodnala SK, Cam M, et al. Identification of essential genes for cancer immunotherapy. Nature. 2017;548:537–42. https://doi.org/10.1038/nature23477.

22. Cazzetta V, Bruni E, Terzoli S, Carenza C, Franzese S, Piazza R, et al. NKG2A expression identifies a subset of human Vδ2 T cells exerting the highest antitumor effector functions. Cell Rep. 2021;37:109871 https://doi.org/10.1016/j.celrep.2021.109871.

23. Reith W, Mach B. The bare lymphocyte syndrome and the regulation of MHC expression. Annu Rev Immunol. 2001;19:331–73. https://doi.org/10.1146/annurev.immunol.19.1.331.

24. Reith W, Siegrist CA, Durand B, Barras E, Mach B. Function of major histocompatibility complex class II promoters requires cooperative binding between factors RFX and NF-Y. Proc Natl Acad Sci USA. 1994;91:554–8. https://doi.org/10.1073/pnas.91.2.554.

25. Masternak K, Barras E, Zufferey M, Conrad B, Corthals G, Aebersold R, et al. A gene encoding a novel RFX-associated transactivator is mutated in the majority of MHC class II deficiency patients. Nat Genet. 1998;20:273–7. https://doi.org/10.1038/3081.

26. Dang AT, Strietz J, Zenobi A, Khameneh HJ, Brandl SM, Lozza L, et al. NLRC5 promotes transcription of BTN3A1-3 genes and Vgamma9Vdelta2 T cell-mediated killing. iScience. 2021;24:101900 https://doi.org/10.1016/j.isci.2020.101900.

27. Stephan A, Wermann M, von Bohlen A, Koch B, Cynis H, Demuth HU, et al. Mammalian glutaminyl cyclases and their isoenzymes have identical enzymatic characteristics. FEBS J. 2009;276:6522–36. https://doi.org/10.1111/j.1742-4658.2009.07337.x.

28. Logtenberg MEW, Jansen JHM, Raaben M, Toebes M, Franke K, Brandsma AM, et al. Glutaminyl cyclase is an enzymatic modifier of the CD47-SIRPalpha axis and a target for cancer immunotherapy. Nat Med. 2019;25:612–9. https://doi.org/10.1038/s41591-019-0356-z.

29. Thompson K, Rogers MJ, Coxon FP, Crockett JC. Cytosolic entry of bisphosphonate drugs requires acidification of vesicles after fluid-phase endocytosis. Mol Pharm. 2006;69:1624–32. https://doi.org/10.1124/mol.105.020776.

30. Yu Z, Surface LE, Park CY, Horlbeck MA, Wyant GA, Abu-Remaileh M, et al. Identification of a transporter complex responsible for the cytosolic entry of nitrogen-containing bisphosphonates. Elife. 2018;7:e36620 https://doi.org/10.7554/eLife.36620.

31. McGilvray PT, Anghel SA, Sundaram A, Zhong F, Trnka MJ, Fuller JR, et al. An ER translocon for multi-pass membrane protein biogenesis. Elife. 2020;9:e56889 https://doi.org/10.7554/eLife.56889.

32. Wainberg M, Kamber RA, Balsubramani A, Meyers RM, Sinnott-Armstrong N, Hornburg D, et al. A genome-wide atlas of co-essential modules assigns function to uncharacterized genes. Nat Genet. 2021;53:638–49. https://doi.org/10.1038/s41588-021-00840-z.

33. Tang Y, Zhou J, Hooi SC, Jiang YM, Lu GD. Fatty acid activation in carcinogenesis and cancer development: Essential roles of long-chain acyl-CoA synthetases. Oncol Lett. 2018;16:1390–6. https://doi.org/10.3892/ol.2018.8843.

34. Kovacs WJ, Tape KN, Shackelford JE, Duan X, Kasumov T, Kelleher JK, et al. Localization of the pre-squalene segment of the isoprenoid biosynthetic pathway in mammalian peroxisomes. Histochem Cell Biol. 2007;127:273–90. https://doi.org/10.1007/s00418-006-0254-6.

35. Vantourout P, Laing A, Woodward MJ, Zlatareva I, Apolonia L, Jones AW, et al. Heteromeric interactions regulate butyrophilin (BTN) and BTN-like molecules governing gammadelta T cell biology. Proc Natl Acad Sci USA. 2018;115:1039–44. https://doi.org/10.1073/pnas.1701237115.

36. Rhodes DA, Chen HC, Williamson JC, Hill A, Yuan J, Smith S, et al. Regulation of Human gammadelta T Cells by BTN3A1 Protein Stability and ATP-Binding Cassette Transporters. Front Immunol. 2018;9:662 https://doi.org/10.3389/fimmu.2018.00662.

37. Wang H, Henry O, Distefano MD, Wang YC, Räikkönen J, Mönkkönen J, et al. Butyrophilin 3A1 plays an essential role in prenyl pyrophosphate stimulation of human Vγ2Vδ2 T cells. J Immunol. 2013;191:1029–42. https://doi.org/10.4049/jimmunol.1300658.

38. Vavassori S, Kumar A, Wan GS, Ramanjaneyulu GS, Cavallari M, El Daker S, et al. Butyrophilin 3A1 binds phosphorylated antigens and stimulates human gammadelta T cells. Nat Immunol. 2013;14:908–16. https://doi.org/10.1038/ni.2665.

39. Riano F, Karunakaran MM, Starick L, Li J, Scholz CJ, Kunzmann V, et al. Vgamma9Vdelta2 TCR-activation by phosphorylated antigens requires butyrophilin 3 A1 (BTN3A1) and additional genes on human chromosome 6. Eur J Immunol. 2014;44:2571–6. https://doi.org/10.1002/eji.201444712.

40. Nguyen K, Li J, Puthenveetil R, Lin X, Poe MM, Hsiao CC, et al. The butyrophilin 3A1 intracellular domain undergoes a conformational change involving the juxtamembrane region. FASEB J. 2017;31:4697–706. https://doi.org/10.1096/fj.201601370RR.

41. Payne KK, Mine JA, Biswas S, Chaurio RA, Perales-Puchalt A, Anadon CM, et al. BTN3A1 governs antitumor responses by coordinating alphabeta and gammadelta T cells. Science. 2020;369:942–9. https://doi.org/10.1126/science.aay2767.

42. Harly C, Guillaume Y, Nedellec S, Peigne CM, Monkkonen H, Monkkonen J, et al. Key implication of CD277/butyrophilin-3 (BTN3A) in cellular stress sensing by a major human gammadelta T-cell subset. Blood. 2012;120:2269–79. https://doi.org/10.1182/blood-2012-05-430470.

43. Willcox CR, Salim M, Begley CR, Karunakaran MM, Easton EJ, von Klopotek C, et al. Phosphoantigen sensing combines TCR-dependent recognition of the BTN3A IgV domain and germline interaction with BTN2A1. Cell Rep. 2023;42:112321 https://doi.org/10.1016/j.celrep.2023.112321.

44. Afrache H, Pontarotti P, Abi-Rached L, Olive D. Evolutionary and polymorphism analyses reveal the central role of BTN3A2 in the concerted evolution of the BTN3 gene family. Immunogenetics. 2017;69:379–90. https://doi.org/10.1007/s00251-017-0980-z.

45. van Diest E, Hernández López P, Meringa AD, Vyborova A, Karaiskaki F, Heijhuurs S, et al. Gamma delta TCR anti-CD3 bispecific molecules (GABs) as novel immunotherapeutic compounds. J Immunother Cancer. 2021;9:e003850 https://doi.org/10.1136/jitc-2021-003850.

46. Lai AY, Patel A, Brewer F, Evans K, Johannes K, González LE, et al. Cutting Edge: Bispecific γδ T Cell Engager Containing Heterodimeric BTN2A1 and BTN3A1 Promotes Targeted Activation of Vγ9Vδ2(+) T Cells in the Presence of Costimulation by CD28 or NKG2D. J Immunol. 2022;209:1475–80. https://doi.org/10.4049/jimmunol.2200185.

47. Kabelitz D, Serrano R, Kouakanou L, Peters C, Kalyan S. Cancer immunotherapy with γδ T cells: many paths ahead of us. Cell Mol Immunol. 2020;17:925–39. https://doi.org/10.1038/s41423-020-0504-x.

48. Mensurado S, Blanco-Domínguez R, Silva-Santos B. The emerging roles of γδ T cells in cancer immunotherapy. Nat Rev Clin Oncol. 2023;20:178–91. https://doi.org/10.1038/s41571-022-00722-1.

49. Mamedov MR, Vedova S, Freimer JW, Sahu AD, Ramesh A, Arce MM, et al. CRISPR screens decode cancer cell pathways that trigger γδ T cell detection. Nature. 2023;621:188–95. https://doi.org/10.1038/s41586-023-06482-x.

COMPETING INTERESTS

WW is a founder and scientific adviser for EdiGene and Therorna, Inc. The other authors declare no competing interests.

ADDITIONAL INFORMATION

Supplementary information The online version contains supplementary material available at https://doi.org/10.1038/s41423-024-01135-z.

Correspondence and requests for materials should be addressed to Catherine CL Wong or Wensheng Wei.

Reprints and permission information is available at http://www.nature.com/reprints